

Article

# Collaborative Methods of Resolving Road Graphic Conflicts Based on Cartographic Rules and Generalization Operations

Chuanbang Zheng <sup>1,\*</sup>, Qingsheng Guo <sup>1,\*</sup>, Lin Wang <sup>2</sup>, Yuangang Liu <sup>3</sup> and Jianfeng Jiang <sup>1</sup>

<sup>1</sup> School of Resources and Environmental Science, Wuhan University, Wuhan 430079, China; zhengcb@whu.edu.cn (C.Z.); jiangjf@whu.edu.cn (J.J.)

<sup>2</sup> Shanghai Surveying and Mapping Institute, Shanghai 200063, China; wanglin\_whu@126.com

<sup>3</sup> School of Geosciences, Yangtze University, Wuhan 430079, China; liuygis@foxmail.com

\* Correspondence: guoqingsheng@whu.edu.cn; Tel.: +86-138-7144-1265

**Abstract:** The resolution of road graphic conflicts is a key aspect of map generalization, which involves both scale reduction and the symbolization of map features. This study proposes collaborative methods of road graphic conflict resolution considering different road characteristics. These methods consider both geometric and semantic characteristics, and they incorporate the bend characteristics of roads, the road symbol size, and road semantics. Constrained Delaunay triangulation skeleton lines are used to categorize road graphic conflicts, which are made up of four independent conflict types and four group conflict types. Based on their characteristics, three collaborative methods are designed to deal with the different types of road graphic conflicts: collaboration between deletion and the snake displacement model, collaboration between the snake displacement model and collinearity, and collaboration among simplification, smoothing, and the beam displacement model. Two types of independent conflicts can be processed using only one simple operation. This study summarizes the cartographic rules for resolving road graphic conflicts, and these are used along with geometric features to drive the collaborative methods or one simple operation presented here. The experimental results indicate that the method proposed in this study can effectively resolve road graphic conflicts.

**Keywords:** cartographic generalization; road graphic conflicts; conflict resolution; cartographic rules; collaborative methods; displacement model



**Citation:** Zheng, C.; Guo, Q.; Wang, L.; Liu, Y.; Jiang, J. Collaborative Methods of Resolving Road Graphic Conflicts Based on Cartographic Rules and Generalization Operations. *ISPRS Int. J. Geo-Inf.* **2024**, *13*, 154. <https://doi.org/10.3390/ijgi13050154>

Academic Editors: Wolfgang Kainz and Florian Hrubý

Received: 15 February 2024

Revised: 8 April 2024

Accepted: 3 May 2024

Published: 6 May 2024



**Copyright:** © 2024 by the authors. Licensee MDPI, Basel, Switzerland. This article is an open access article distributed under the terms and conditions of the Creative Commons Attribution (CC BY) license (<https://creativecommons.org/licenses/by/4.0/>).

## 1. Introduction

Road generalization is an important research direction in the field of map generalization [1–3]. It mainly includes road selection [4,5], road simplification [6,7], road pattern recognition [8], and road displacement [9–11]. Graphic conflicts are drivers of road generalization after road symbolization in the process of reducing the map scale [12]. Graphic conflict resolution is one of the challenges for automatic cartographic generalization [13]. The clear representation of roads on a map necessitates the resolution of graphic conflicts. Displacement is considered the main operation in the resolution of graphic conflicts in map generalization. Ai [14] used the concept of vector fields to execute polygonal target group displacement while considering contextual factors. Burghardt and Meier [15] first introduced the snake displacement model in cartographic generalization for curve displacement, and Bader [9] proposed the beam displacement model. Snake and beam displacement models have been employed to address road and building generalization [10,16–20].

Wang [17] divided displacement methods into continuous geometry and optimization methods. Continuous geometry methods handle spatial conflicts on a case-by-case basis by using a displacement method. Nickerson [21] proposed a road displacement method by using a buffer to detect graphic conflicts. Fei [22] used a displacement operation to resolve graphic conflicts between streets and buildings on a map. Optimization methods resolve graphic conflicts from a global perspective, for example, with the snake and beam

displacement models [16–20]. Ware and Jones [23] used a simulated annealing approach to perform displacement operations and resolve graphic conflicts. Subsequently, Ware, Jones, and Thomas [24] improved this approach by considering generalization operations such as displacement, deletion, exaggeration, and reduction. However, displacement algorithms alone cannot solve all graphic conflicts when there is insufficient map space for displacement.

In recent years, different generalization operators and algorithms have been combined to create effective cartographic generalization approaches driven by map generalization rules, such as a series of collaborative model generalization methods developed based on agent models [25–31]. Li [32] proposed a collaborative method by combining three cartographic generalization operations to resolve the spatial conflicts between buildings and other features in urban villages. Thus, collaborative ideas should be an effective approach to resolving graphic conflicts.

This study proposes collaborative methods for resolving different types of road graphic conflicts. The main contributions of this study are as follows:

- (1) Road graphic conflicts can be automatically categorized into eight types: four independent conflict types and four group conflict types, which provides a basis for their resolution.
- (2) Three collaborative methods were designed to deal with different types of road graphic conflicts, namely, collaboration between deletion and the snake displacement model, collaboration between the snake displacement model and collinearity, and collaboration among simplification, smoothing, and the beam displacement model.
- (3) The cartographic rules for resolving road graphic conflicts are summarized and used to drive the collaborative methods or one simple operation.

This study is organized as follows: the methodology is introduced in Section 2, which includes the recognition and classification of road graphic conflicts, collaborative methods for road graphic conflicts, and cartographic rules for resolving graphic conflicts. The experiments and analysis are reported in Section 3 with experimental illustrations. The main conclusions of the work are provided in Section 4.

## 2. Methodology

After the map scale is reduced, road graphic conflicts arise when roads are symbolized. Not all road graphic conflicts can be resolved using only one operation [10,17]. Therefore, it is crucial to determine which operation or operations are used to resolve different types of road graphic conflicts. When multiple operations must be used at the same time, these operations must work together to process the data in the road conflict area. The completion of a specific map generalization task often necessitates the combination of several operations [33]. A data processing workflow based on collaborative methods for resolving road graphic conflicts is shown in Figure 1, and the following are the main methods proposed in this study.

- (1) Road graphic conflicts are recognized and classified, and the characteristics of the conflict areas are calculated. According to the average distance between the skeleton lines in road graphic conflict areas, conflicts are classified as independent conflicts or group conflicts, which are each further subdivided into four subclasses based on the relevant characteristics of the skeleton lines in the conflict areas. Each subclass corresponds to a collaborative method or an operation.
- (2) According to the type of road graphic conflict, simple operations are used individually or cooperatively. Simple operations for resolving road graphic conflicts include deletion, displacement, collinearity, smoothing, and simplification. The collaborative methods designed in this study include collaboration between deletion and the snake displacement model, collaboration between the snake displacement model and collinearity, and collaboration among simplification, smoothing, and the beam displacement model. Cartographic rules for resolving road graphic conflicts are established with reference to cartographic specifications and conditions, which establish

correspondences between the type of road graphic conflict and the use of simple operations or collaborative methods.

- (3) It is judged whether there are subsequent graphic conflicts in the generated map, and, if so, it is necessary to rejudge the type of road graphic conflict and continue to resolve it. The process is repeated until there are no subsequent graphic conflicts in the generated map.

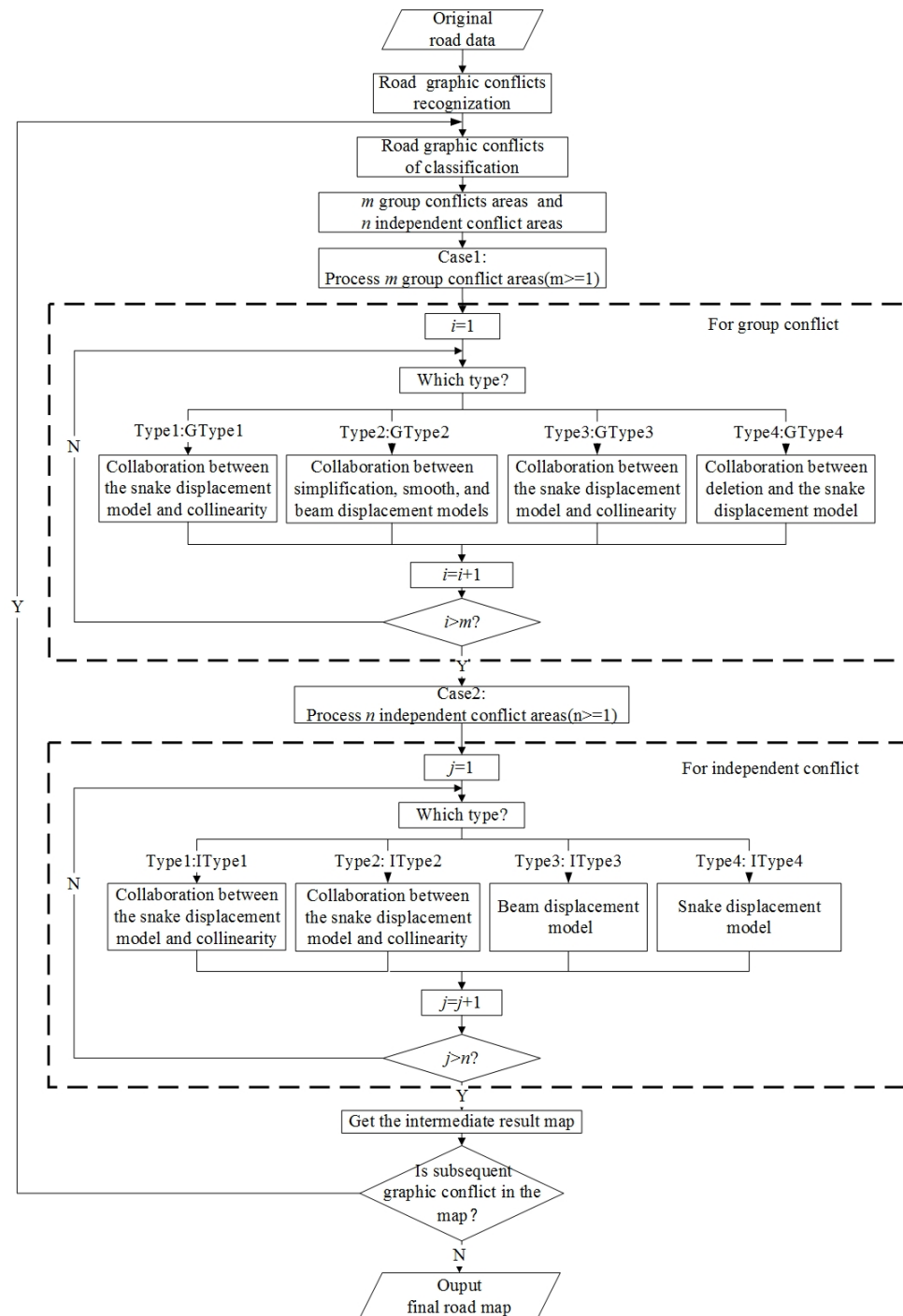


Figure 1. Data processing workflow based on collaborative methods.

## 2.1. Recognition and Classification of Road Graphic Conflicts

It is necessary to first identify road graphic conflict areas. Constrained Delaunay triangulation (CDT) is widely used in cartographic generalization for neighborhood calculations and spatial conflict detection [34,35]; road graphic conflicts are detected by extracting skeleton lines through CDT, and information on the relevant road characteristics is calculated to assist in the resolution of road graphic conflicts.

### 2.1.1. Conflict Recognition and Characteristic Information Calculation

Based on the road centerline and the road symbol width, road symbol borderlines can be generated. Using the road centerline and its road symbol borderlines as constraint edges, constrained Delaunay triangulation (CDT) can be applied. Skeleton line extraction methods based on CDT can be used to identify graphic conflicts on roads [10,17]; each road graphic conflict area can be represented by its skeleton line. The triangles in CDT can be categorized into 11 types, as seen in Figure 2, considering the numbers of triangle edges and triangle vertices located on road symbol borderlines or road centerlines.  $R_{mn}$  indicates the classification of triangles, where  $m$  indicates the total number of constrained triangle edges, and  $n$  indicates the  $n$ th subtype of the  $m$ th type.

All triangles crossed by the skeleton line in a conflict area form a triangular path. If one of two triangles located at the ends of a triangular path belongs to the  $R_{2n}$  type, then the triangle is called EnT, the last triangle on this triangular path is called ExT, and all triangles between EnT and ExT along this triangular path are called MT.

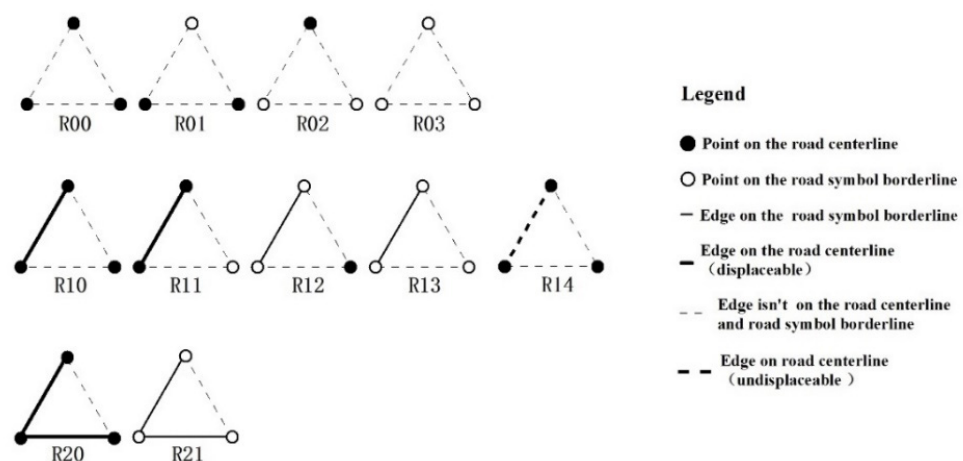


**Figure 2.** Classification of triangles in CDT for roads.

After extracting a skeleton line in a road graphic conflict area, it is necessary to determine its direction and correlative points. If the endpoint of the skeleton line is not a vertex of triangle  $R_{2n}$ , then the perpendicular points from that endpoint to the constrained edges on the left and right sides of that skeleton line must be calculated. For example, as shown in Figure 3a,  $P_{L1}$  and  $P_{L2}$  are the left correlative points of skeleton line  $S_1$ ;  $P_{R1}$  and  $P_{R2}$  are the right correlative points of skeleton line  $S_1$ ; and  $P_L$  and  $P_R$  are the left correlative point and right correlative point of skeleton line  $S_2$ , respectively.

If the endpoint of the skeleton line is a vertex of triangle  $R_{2n}$ , the section of the road centerline in the road graphic conflict area represented by this skeleton line is defined as a bottleneck road segment (BRS), whereas the sections of road centerlines in road graphic conflict areas represented by other types of skeleton lines are defined as curved road segments (CRSs). For example, as shown in Figure 3a, the road centerline in the road graphic conflict area represented by  $S_2$  from  $P_L$  to  $P_R$  is a CRS, whereas those road centerlines from  $P_{L1}$  to  $P_{L2}$  and from  $P_{R2}$  to  $P_{R1}$  are BRSs in the road graphic conflict area represented by  $S_1$ .

A polygon enclosed by a road symbol borderline may be connected with two skeleton lines, for example, polygon  $C_1$  in Figure 3a and polygon  $C_2$  in Figure 3b. If the area of this polygon is less than the area threshold, then the main skeleton line of this polygon must be extracted [10,17], and this main skeleton line must be connected with two other skeleton lines connected to this polygon to form a complete skeleton line, such as skeleton line  $S_0$  in Figure 3c. If the area of the polygon is greater than the area threshold, then the main skeleton line of this polygon cannot be extracted, as shown in Figure 3b.

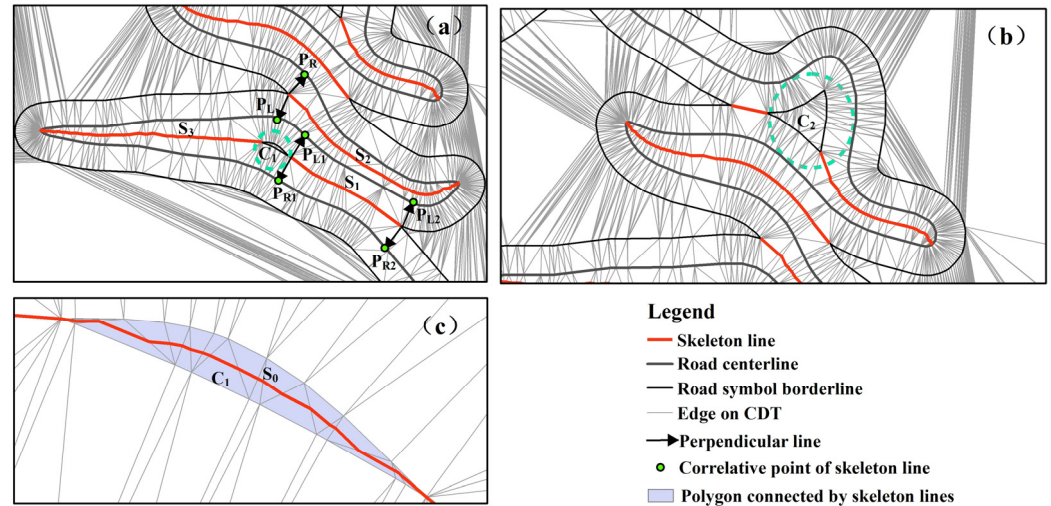


**Figure 3.** Connection between a bottleneck road segment and a curved road segment. (a) BRS and CRS; (b) the case skeleton lines are not connected; (c) the case skeleton lines are connected.

The length of the skeleton line ( $L_{sk}$ ) and the average width of the road graphic conflict area ( $W_{sk}$ ) are calculated with Formulas (1) and (2), respectively, in which  $L_{sk}$  and  $W_{sk}$  depend on the types of triangles crossed by the skeleton line

$$L_{sk} = \sum_{i=1}^j \|N_i N_{i+1}\|, \tag{1}$$

where,  $\|N_i N_{i+1}\|$  represents the length of the line connecting point  $N_i$  and point  $N_{i+1}$  in a triangle, and  $1 \leq i \leq j$ , where  $j$  represents the number of triangles crossed by the skeleton line. For example, as shown in Figure 4,  $N_1$  and  $N_{j+1}$  represent the vertex of EnT and ExT in A and B, respectively;  $N_2$ ,  $N_i$ ,  $N_{i+1}$ , and  $N_j$  represent the midpoint of the edges of EnT, MT, and ExT in A, B, and C, respectively,

$$W_{sk} = \sum_{i=1}^j \frac{\|N_i N_{i+1}\| W_i}{L_{sk}}, W_i = \|W_{i1} W_{i2}\|, \tag{2}$$

where,  $\|W_{i1} W_{i2}\|$  represents the length of the line connecting point  $W_{i1}$  and point  $W_{i2}$  in a triangle. For example, as shown in Figure 4,  $W_{11}$ ,  $W_{12}$ ,  $W_{j1}$ , and  $W_{j2}$  represent the midpoint of the edges of EnT and ExT in A and C, respectively,  $W_{i2}$  represents the vertex of MT, and  $W_{i1}$  represents the perpendicular point from  $W_{i2}$  to the edge of MT.

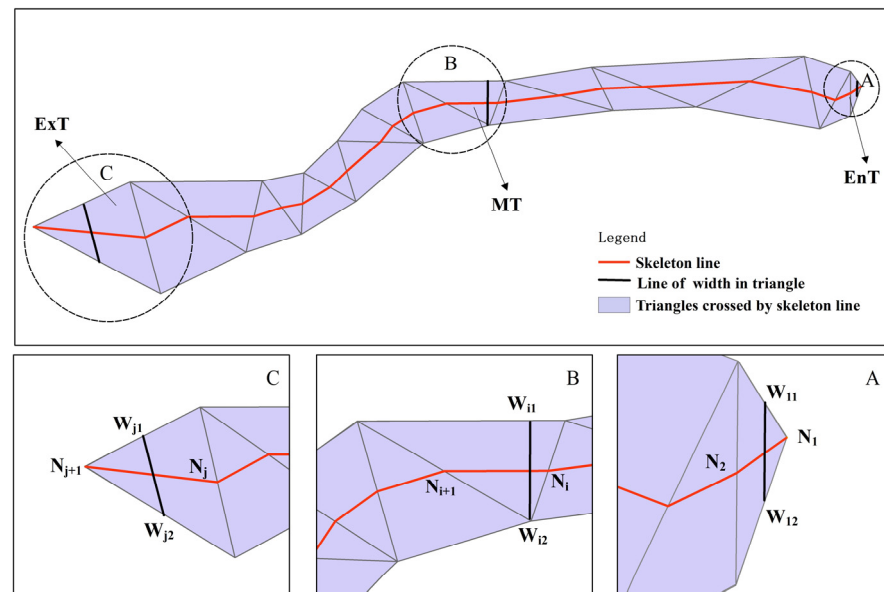


**Figure 4.** Calculation of the skeleton line length and the average width of a road conflict area. A: EnT; B: MT; C: ExT.

### 2.1.2. Conflict Types

When graphic conflict areas interact with each other, it becomes necessary to group them together. Whether two graphic conflict areas interact with each other can be determined by the average distance between their two skeleton lines. The threshold of this average distance,  $T_p$ , is calculated with Formula (3):

$$T_p = W_{rs} + D_{ms}/2, \quad (3)$$

where  $W_{rs}$  represents the width of the road symbol, and  $D_{ms}$  represents the minimum distance between map objects. When the distance between the skeleton line of a conflict area and that of a neighboring conflict area is greater than  $T_p$ , it is regarded as an independent conflict type (called an IC).

If the average distance between a skeleton line and other skeleton lines is greater than the distance threshold, then the graphic conflict area represented by that skeleton line is an IC. The following are the four different types of ICs:

- (1) For IType1, the first endpoint or last endpoint of the skeleton line is one vertex on the road centerline, and another endpoint is one vertex on the road symbol borderline, as shown in Figure 5a.
- (2) For IType2, the first endpoint and last endpoint of the skeleton line are on the road symbol borderline, as shown in Figure 5b.
- (3) For IType3, the first endpoint and last endpoint of the skeleton line are not on the road centerline and the road symbol borderline. One road segment corresponding to the skeleton line of the conflict area is displaceable, as shown in Figure 5c.
- (4) For IType4, the first endpoint and last endpoint of the skeleton line are not on the road centerline and the road symbol borderline. Two road segments corresponding to the skeleton line of the conflict area are displaceable, as shown in Figure 5d.

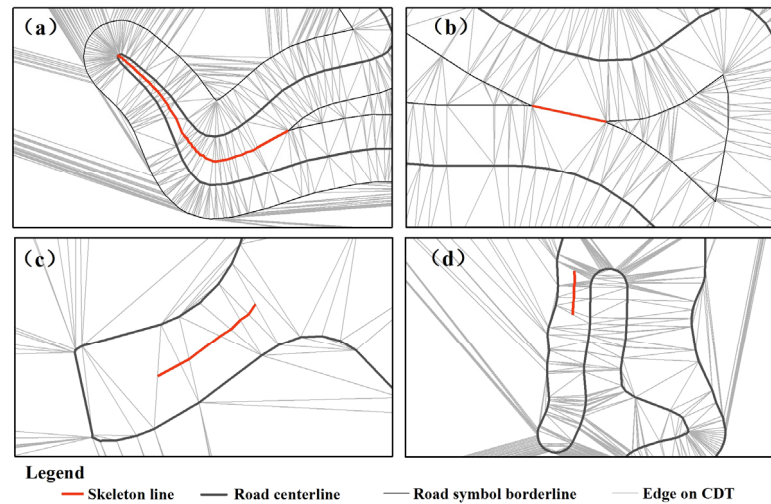


Figure 5. Independent conflict types: (a) IType1, (b) IType2, (c) IType3, and (d) IType4.

If the average distance of a skeleton line from other skeleton lines is smaller than the threshold value, then the graphic conflict areas represented by these skeleton lines are a group conflict and are called GC. If any two adjacent skeleton lines are among all the skeleton lines in a GC area and a correlative point of one of two adjacent skeleton lines lies between two correlative points of the other skeleton line, then this GC area is called a collinear curved group; otherwise, this GC area is called a non-collinear curved group. For example, as shown in Figure 6a, a correlative point  $P_{L1}$  of one skeleton line  $S_1$  is between two correlative points  $P_{L2}$  and  $P_{R2}$  of the other skeleton line  $S_2$ ; therefore, it is a collinear curved group. There are four types of GCs, which are as follows:

- (1) If the GC area is a collinear curved group and the number of skeleton lines is even, it is GType1, as seen in Figure 6a.
- (2) If the GC area is a collinear curved group and the number of skeleton lines is odd, it is GType2, as seen in Figure 6b.
- (3) If the GC area is a non-collinear curved group, it is GType3, as seen in Figure 6c.
- (4) If there are both non-collinear curved and collinear curved groups in the GC area, it is GType4, as seen in Figure 6d.

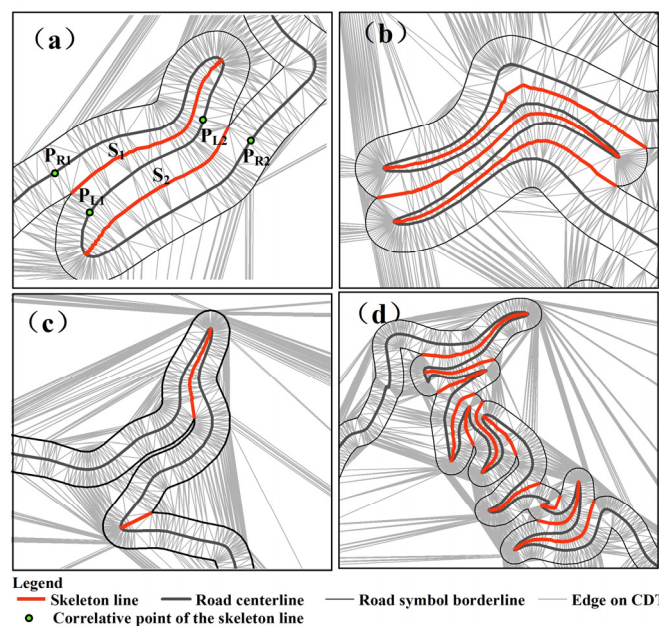


Figure 6. Group conflict types: (a) GType1, (b) GType2, (c) GType3, and (d) GType4.

## 2.2. Collaborative Methods

It is necessary to choose a collaborative method according to the type of graphic conflict. Three collaborative methods are proposed in this study: collaboration between deletion and the snake displacement model, collaboration between the snake displacement model and collinearity, and collaboration among simplification, smoothing, and the beam displacement model.

### 2.2.1. Cartographic Rules for the Resolution of Road Graphic Conflicts

Cartographic rules can be used to guide conflict resolution; they include the order of handling different conflicts, the order of applying operations, the conditions of using operations, and the constraints on mapping specifications. Li [36] proposed a classification scheme for map generalization operators considering the geometric properties of map objects. Regnauld and McMaster [37] provided a framework for map generalization operators. Stanislawski et al. summarized the map generalization operators associated with network generalization [13]. Simple operations and their corresponding algorithms for resolving road graphic conflicts selected in this study are shown in Table 1. The cartographic rules used in this study for road graphic conflict resolution are summarized in Table 2. For example, when dealing with different types of independent conflicts, it is necessary to follow  $R_{S1}$  and  $R_{S2}$  to determine which conflict area should be dealt with in which order. When dealing with different types of group conflicts,  $R_{O1}$ – $R_{O3}$  can be used to decide which collaborative method should be selected.

**Table 1.** Simple operations and the corresponding algorithms.

Operations	Algorithm
Smoothing	Peak (from ArcGIS)
Displacement	Snake [17], beam [10]
Collinearity	Collinearity method [17]
Simplification	Algorithm proposed in this study
Deletion	Algorithm proposed in this study

**Table 2.** Cartographic rules for road graphic conflict resolution.

Number	Description of Cartographic Rules
$R_{S1}$	If $\exists$ IType1 and $\exists$ IType2, then IType2 should be processed first.
$R_{S2}$	If $\exists$ IType3 and $\exists$ IType4, then IType4 should be processed first.
$R_{S3}$	If $\exists$ IC and GC, then GC should be processed first.
$R_{O1}$	If $W_{rs} <$ the required width of a GC $<$ the maximum allowable displacement threshold, then operation = collaboration between the snake displacement model and collinearity.
$R_{O2}$	If the required width of a GC $>$ the maximum allowable displacement threshold and the current width of a GC $<$ $W_{rs}$ , then operation = collaboration among simplification, smoothing, and the beam displacement model.
$R_{O3}$	If the required width of a GC $>$ the maximum allowable displacement threshold and the current width of a GC $>$ $W_{rs}$ , then operation = collaboration between deletion and the snake displacement model.
$R_{O4}$	If $L_{sk}$ in CRS $<$ $W_{rs}$ , then operation = displacement; otherwise, operation = collaboration between the snake displacement model and collinearity.
$R_{O5}$	If $\exists$ IType3, then operation = beam displacement; if $\exists$ IType4, then operation = snake displacement.
$R_{C1}$	If operation = displacement, then the displacement magnitude is $<0.5$ mm.
$R_{C2}$	If $\exists$ any graphic conflict, then $D_{ms} < 0.2$ mm.

## 2.2.2. Collaboration between Deletion and the Snake Displacement Model

If the width of a group conflict area is not sufficient to resolve a graphic conflict based only on the displacement operation and the length difference of the skeleton lines in this group conflict area is larger than a certain threshold, then the deletion operation and the snake displacement model must be used in collaboration.

The skeleton line set of this group conflict area is represented as  $S = \{S_1, S_2, \dots, S_n\}$ , and  $n$  represents the number of skeleton lines in this group conflict area. A subset of the vertexes on the road centerline is represented as  $V = \{V_0, V_1, V_2, \dots, V_n, V_{n+1}\}$ , where  $V_0$  and  $V_{n+1}$  represent the correlative points of  $S_1$  and  $S_n$  on this road centerline, respectively, according to the method mentioned in Section 2.1.1.  $V_1, V_2, \dots, V_n$  represent the respective intersections between the road centerline and each skeleton line  $S_i$ ;  $V_{i(i+1)}$  represents the midpoint on the road centerline between  $V_i$  and  $V_{i+1}$  ( $1 \leq i \leq n$ ); a set of the midpoints is represented as  $V_{\text{mid}} = \{V_{12}, V_{23}, \dots, V_{(n-1)n}\}$ . For example, as shown in Figure 6a,  $S = \{S_1, S_2, S_3, S_4, S_5, S_6, S_7\}$ ,  $V = \{V_0, V_1, V_2, V_3, V_4, V_5, V_6, V_7, V_8\}$ , and  $V_{\text{mid}} = \{V_{12}, V_{23}, V_{34}, V_{45}, V_{56}, V_{67}\}$ . The current width ( $W_c$ ) and the required width ( $W_r$ ) of this group conflict area are calculated with Formula (4) and Formula (5), respectively:

$$W_c = \sum_{i=1}^n W_{sk(i)}, \quad (4)$$

$$W_r = n * (W_{rs} + D_{ms}), \quad (5)$$

where  $W_{sk(i)}$  represents the average width of this group conflict area through which the  $i$ -th skeleton line passes, as mentioned in Section 2.1.1.  $W_{rs}$  represents the width of the road symbol, and  $D_{ms}$  represents the minimum spacing distance determined by rule RC2.

The length difference of these skeleton lines is expressed as the standard deviation ( $\sigma_L$ ), which is calculated with Formula (6):

$$\sigma_L = \sqrt{\frac{\sum_{i=1}^n (L_i - \bar{L})^2}{n}}, \quad (6)$$

where the set of lengths of these skeleton lines in this group conflict area is represented as  $L = \{L_1, L_2, L_3, L_4, \dots, L_n\}$ ,  $L_i$  represents the length of the  $i$ -th skeleton line, and  $\bar{L}$  represents the average length of these skeleton lines. The maximum displacement distance ( $D_{md}$ ) can be determined by rule RC1. If  $W_r - W_c > D_{md}$  and if  $\sigma_L$  is larger than a certain threshold, then the width of this group conflict area is not sufficient to resolve the graphic conflict based only on the displacement operation, and the deletion operation and the snake displacement model must instead be used in collaboration.

The deletion operation involves deleting part of a road centerline, which is the road segment that corresponds to the shortest skeleton line and its adjacent skeleton line in the group conflict area.

Because the visual symmetry of road bends should be considered from the perspective of visual perception, it is assumed that  $S_m$  is used to represent the shortest skeleton line in  $\{S_1, S_2, \dots, S_n\}$ , and its adjacent skeleton line is  $S_{m-1}$  or  $S_{m+1}$ . The three cases for deleting this road segment are as follows:

- (1) If  $1 < m < n$ , then it is necessary to select the adjacent skeleton line of  $S_m$ . If  $L_{m-1} < L_{m+1}$ , then the selected adjacent skeleton line is  $S_{m-1}$ ; otherwise, the selected adjacent skeleton line is  $S_{m+1}$ . For example, if  $S_5$  is the shortest skeleton line, the road segment that corresponds to  $S_5$  is the road centerline from  $V_{45}$  to  $V_{56}$ , as seen in Figure 7a. If  $S_4$  and  $S_6$  are the skeleton lines adjacent to  $S_5$ ,  $S_6$  is selected as  $S_5$ 's adjacent skeleton line, as  $L_6 < L_4$ . The road segment that corresponds to  $S_6$  is the road centerline from  $V_{56}$  to  $V_{67}$ , as seen in Figure 7a. Therefore, the road segment from  $V_{45}$  to  $V_{67}$  in Figure 7a is deleted.
- (2) If  $m = 1$ , then the only adjacent skeleton line of  $S_1$  that can be selected is  $S_2$ , and the road segment from  $V_0$  to  $V_{12}$  is deleted.

- (3) If  $m = n$ , then the only adjacent skeleton line of  $S_n$  that can be selected is  $S_{n-1}$ , and the road segment from  $V_{(n-1)n}$  to  $V_{n+1}$  is deleted.

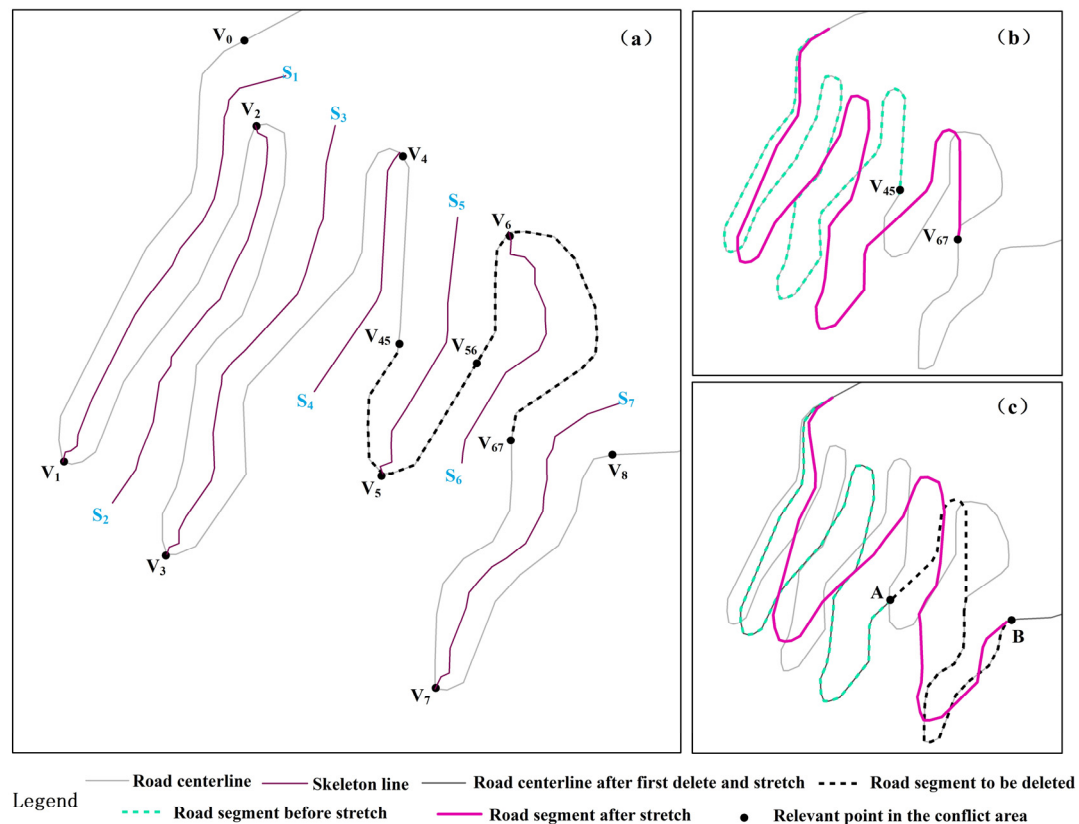


**Figure 7.** The process of collaboration between the deletion operation and the snake displacement model: (a) finding the first deleted road segment; (b) the first collaboration between the deletion operation and the snake displacement model; (c) the second collaboration between the deletion operation and the snake displacement model, A represents the midpoint of two intersections and B represents the correlative point of the skeleton line.

To maintain the graphic characteristics of the remaining road segments in the group conflict area, the snake displacement model [17] is used to stretch these segments. The stretching direction is determined by comparing the  $W_r$  values of the two road segments on either side of the deleted road segment. If the  $W_r$  value of one road segment (RS) is larger than the other, the direction of the stretch is from the road segment (RS) to the other road segment. For example, the stretching direction is from  $V_{45}$  to  $V_{67}$  in Figure 7b. Sometimes only one collaboration between the deletion operation and the snake displacement model is not sufficient to meet the requirement of resolving a graphic conflict; therefore, the collaboration must be used several times, and the number of iterations ( $N_{it}$ ) of this collaboration can be calculated with Formula (7). For example, Figure 7c is the result after the second collaboration, where the stretching direction is from point A to point B:

$$N_{it} = \lceil (W_r - W_c) / W_{rs} \rceil, \quad (7)$$

where  $W_c$  and  $W_r$  are calculated with Formula (4) and Formula (5), respectively.

If  $\sigma_L$  is less than a certain threshold, after determining  $N_{it}$ , the road segment on one side in the group conflict area is arbitrarily deleted, and then the remaining road segment is stretched.

### 2.2.3. Collaboration between the Snake Displacement Model and Collinearity

If the difference between the required width and the current width of a group conflict area is less than the maximum displacement distance, then a collaboration between the snake displacement model and collinearity is used.

The skeleton line set of this group conflict area is represented as  $S = \{S_1, S_2, \dots, S_n\}$ , and  $n$  represents the number of skeleton lines in this group conflict area. A subset of the correlative points of skeleton lines on the road centerline is represented as  $R = \{R_1, R_2, R_3, \dots, R_{2n}\}$ . The two methods for the collaboration between displacement and collinearity are as follows:

- (1) If the correlative point of one skeleton line is not between the positions of two correlative points of another skeleton line, then the collinearity [17] is used to resolve the conflict represented by each skeleton line according to the road symbol width. For example, in Figure 8a,  $R_3$  is not between  $R_1$  and  $R_2$ , and  $R_2$  is not between  $R_3$  and  $R_4$ . To ensure that a smoother connection can be made at the correlative points, it is necessary to use the displacement operation for displacement propagation after the collinearity, as seen in Figure 8b. The snake [17] model is used to deal with non-collinear portions of road segments that are connected to correlative points of a skeleton line, as seen in Figure 8b.

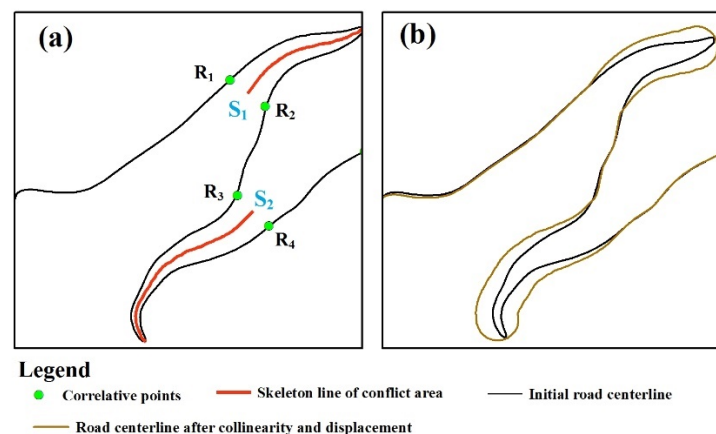


**Figure 8.** Collaboration between the snake displacement model and collinearity. (a) extraction of skeleton line of conflict area; (b) collaboration between the snake displacement model and collinearity.

- (2) If the correlative point of one skeleton line is between the positions of two correlative points of another skeleton line (e.g.,  $R_2$  is between  $R_1$  and  $R_3$  in Figure 9a), then the snake displacement model [17] is used to displace one of the two neighboring skeleton lines (e.g.,  $S_3$  is displaced to  $S_3'$  in Figure 9b). The parallel line AB of skeleton line  $S_4$  is obtained according to the width of the road symbol. O is the nearest point from endpoint E of  $S_3$  to AB in Figure 9c; P is the nearest point from point B to skeleton line  $S_3'$ ; and C and D are endpoints of  $S_3'$  in Figure 9d. The line PD is shifted to let P coincide with point B, and then it is connected with OB so as to obtain line  $S_3''$  in Figure 9e, and the collinearity [17] operation is applied to  $S_3''$  and  $S_4$ . The snake [17] model is used to deal with non-collinear portions of road segments that are connected to correlative points of a skeleton line. For example,  $R_1$  and  $R_4$  are correlative points, as shown in Figure 9f.

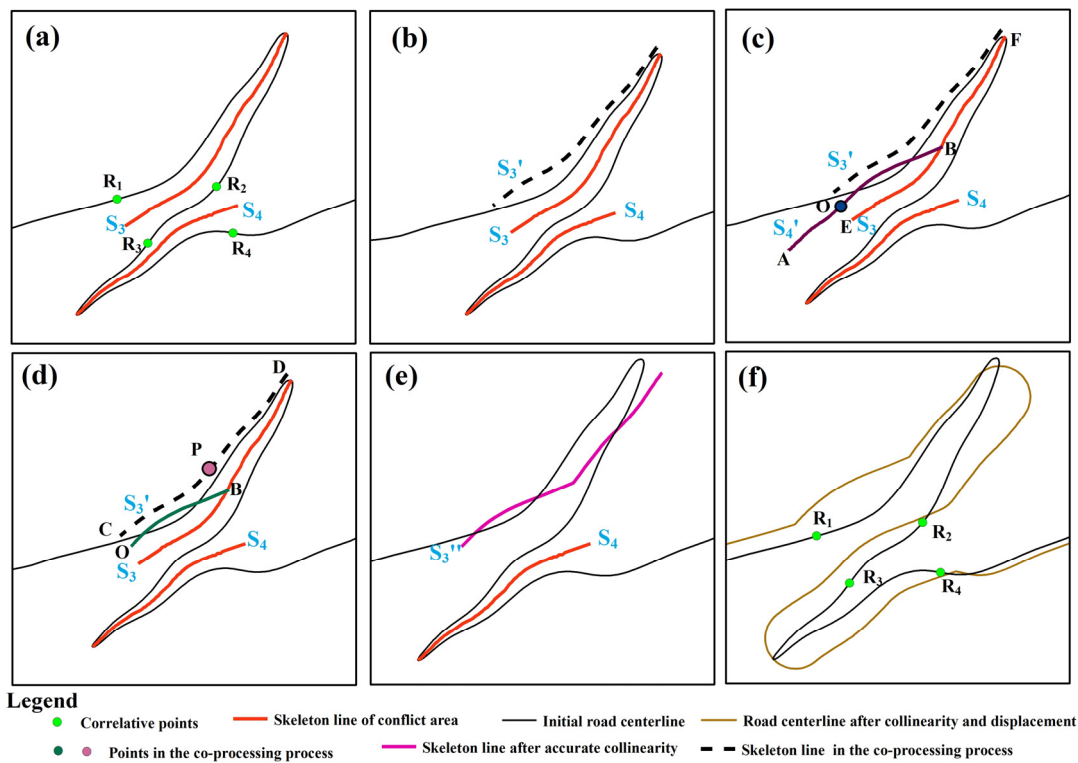


**Figure 9.** Collaboration between the snake displacement model and collinearity. (a) extraction of skeleton line of conflict area; (b) displace one of the two neighboring skeleton lines; (c) the parallel line AB of skeleton line  $S_4$  is obtained; (d) get the nearest point P from point B to skeleton line  $S_3'$ ; (e) obtain line  $S_3''$ ; (f) the collinearity operation is applied to  $S_3''$  and  $S_4$ , and the snake model is used to deal with non-collinear portions of road segments.

#### 2.2.4. Collaboration among Simplification, Smoothing, and the Beam Displacement Model

If the width of a group conflict area is not sufficient to resolve a graphic conflict based on collaboration between displacement and collinearity or collaboration between deletion and the snake displacement model, then the simplification operation and collaboration must be used.

The skeleton line set of this group conflict area is represented as  $S = \{S_1, S_2, \dots, S_n\}$ , and  $n$  represents the number of skeleton lines in this group conflict area. A subset of the vertexes on the road centerline is represented as  $V = \{V_0, V_1, V_2, \dots, V_n, V_{n+1}\}$ , where  $V_0$  and  $V_{n+1}$  represent the correlative points of  $S_1$  and  $S_n$  on this road centerline, respectively, according to the method mentioned in Section 2.1.1;  $V_1, V_2, \dots, V_n$  represent the intersections between the road centerline and each skeleton line  $S_i$ . The two cases for the simplification operation are as follows:

- (1) If  $n$  is even, all road segments in the road graphic conflict area are deleted, and then the two correlative points of the outermost skeleton line on the road centerline are connected. For example, as shown in Figure 10a, a part of the road centerline from the correlative point  $V_0$  of skeleton line  $S_1$  to the correlative point  $V_5$  of skeleton line  $S_4$  is deleted in the group conflict area, and then  $V_0$  and  $V_5$  are connected; the result is shown in Figure 10b. After the simplification operation, if there are sharp corners at the connection of the road centerline, then the smoothing operation is used to remove them.

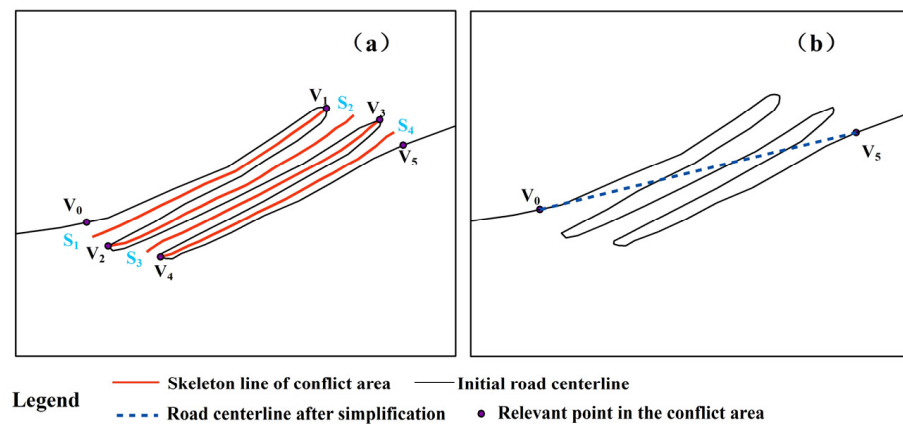


**Figure 10.** Process of simplification and its collaboration: (a) extraction of skeleton line of conflict area; (b) simplification and its collaboration.

- (2) If  $n$  is odd, the road segment from the first intersection to the last intersection in the group conflict area is deleted, and then the two intersections are connected. For example, in Figure 11a, a part of the road centerline from  $V_1$  to  $V_3$  is deleted, and then  $V_1$  and  $V_3$  are connected in the group conflict area. After the simplification operation, if there are sharp corners at the connection of the road centerline, then the smoothing operation is also required to remove them, as seen in Figure 11b. If there are still conflicts after simplification, the beam displacement model [10] is used with collaborative displacement to expand the width of the external space and resolve the conflict, as seen in Figure 11c.

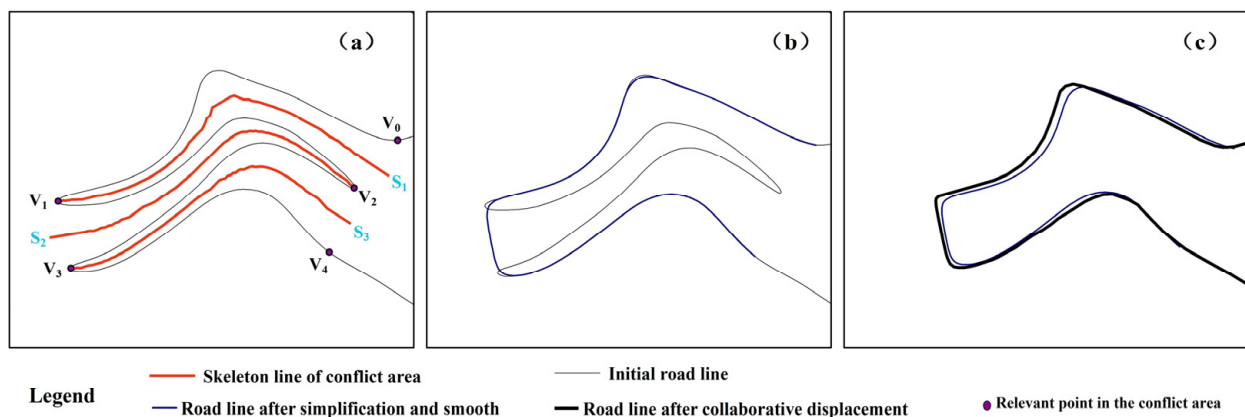


**Figure 11.** The process of simplification and its collaboration: (a) conflict area, (b) simplification and smoothing operations, and (c) the beam displacement model for collaborative displacement.

### 3. Experiments and Analysis

#### 3.1. Experimental Data and Related Parameters

Experimental data on Sichuan Province, China were downloaded from OpenStreetMap (OSM) at <https://www.openstreetmap.org/> (accessed on 2 May 2024). The scale of these experimental data was 1:10,000, as shown in Figure 12. Figure 13 shows the road map after symbolization, and the width of the road symbols on the map was from 0.6 to 1.2 mm for different types of roads. The total length of road centerlines in the experimental dataset was 24.36 km on the Earth. The scale of Figure 13 is 1:50,000.

The software for the methods proposed in this study was developed using C# in vs 2015 and the ArcGIS Engine, and the hardware was a PC with Windows 10 OS and an Intel(R) Core(TM) i5-4460 CPU (3.20 GHz). The total runtime of this software for processing these experimental data was 378 s.

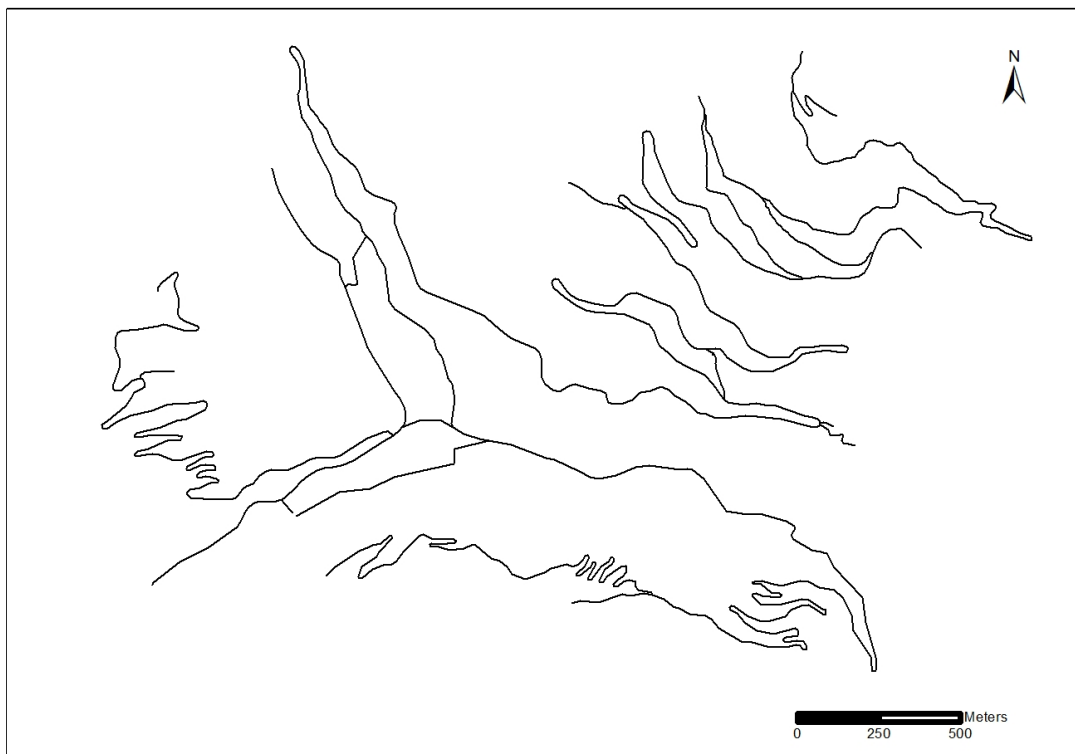


Figure 12. Experimental data.

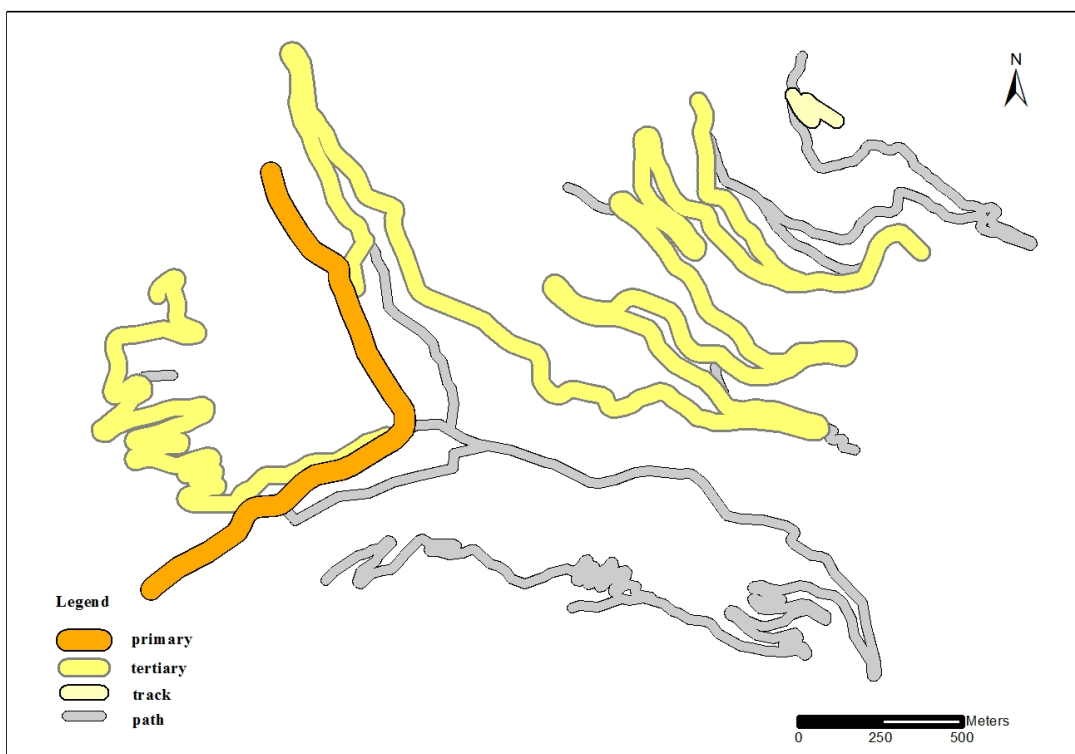


Figure 13. Road map after symbolization.

### 3.2. Experimental Results and Analysis

Figure 14 shows the skeleton lines that were extracted in the road graphic conflict areas in the experimental data. There were eight group conflict areas and nine independent conflict areas, as shown in Figure 14. The group conflict areas in Figure 14 were resolved

with the three collaborative methods, and the independent conflict areas were resolved through collinearity and displacement. The final road map is shown in Figure 15.

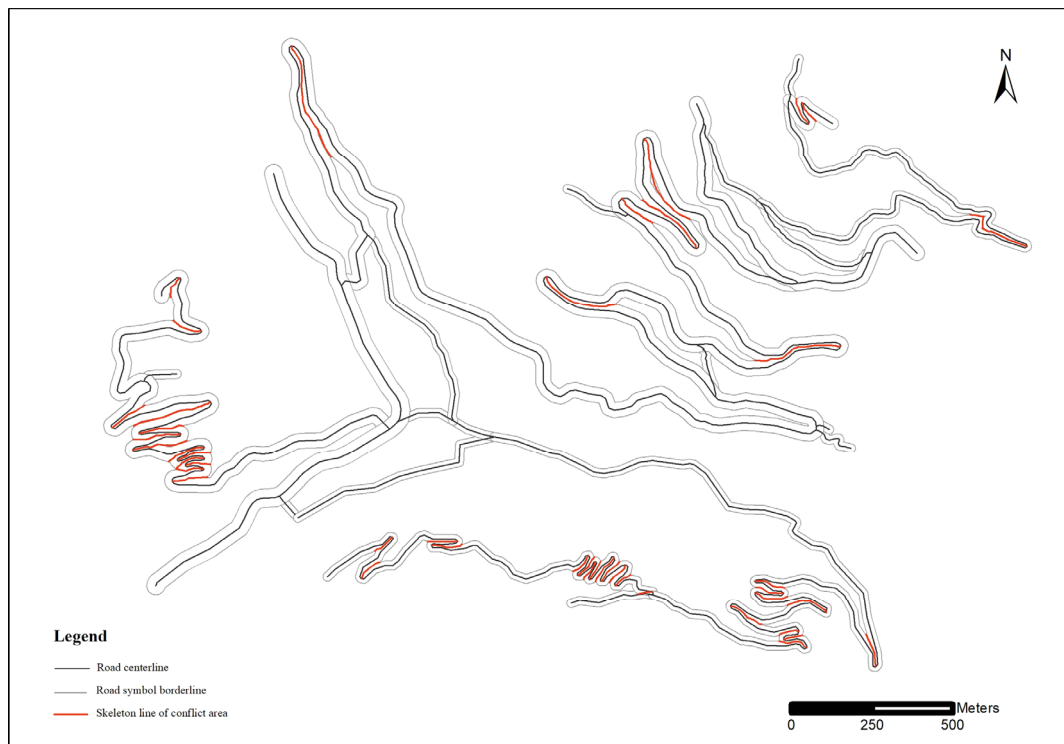


Figure 14. Map of road graphic conflict areas.

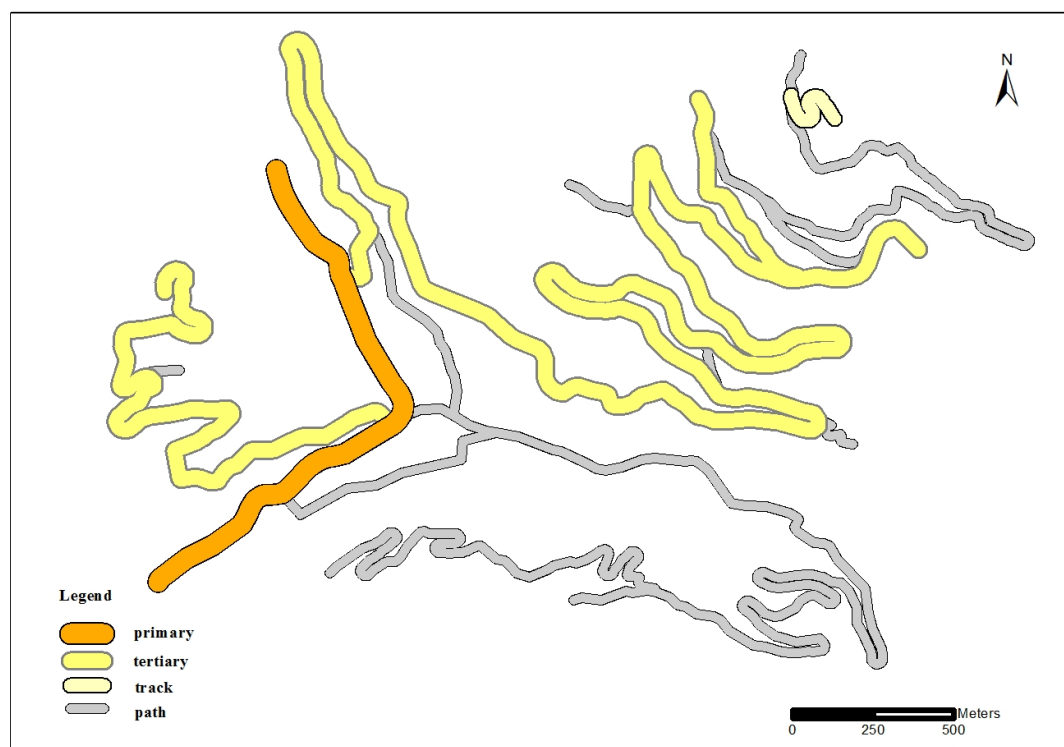
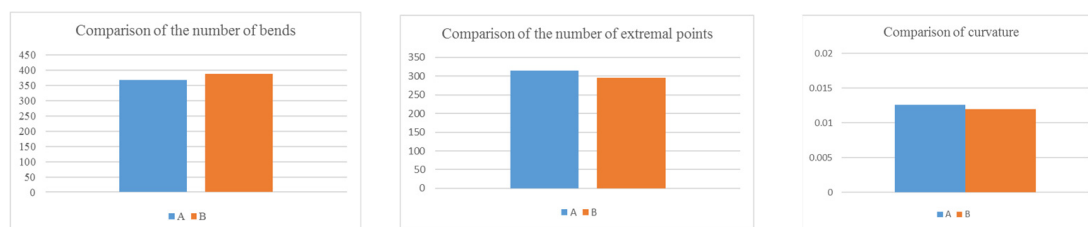


Figure 15. The final road map.

The experimental results in Figure 15 meet the requirements for visual clarity, and there are no visual conflicts. Some indicators were used to evaluate the degree of conflict

resolution: the displacement magnitudes of the vertexes, the coalescence strength, and the shape measures of the roads.

- (1) The displacement magnitudes of vertexes: The specification in [38] requires that the maximum displacement magnitude of vertexes is from 0.5 to 1 mm on a map, but the maximum displacement magnitude of vertexes in this experimental result was <0.3 mm.
- (2) Coalescence strength: After calculating the total actual area (A1) of buffers of roads on the map at a scale of 1:50,000 and the total ideal area (A2) of map symbols for these roads, the coalescence strength can be represented as  $1 - A1/A2$  [39]. The coalescence strength of this road map was 0.003, which was smaller than 0.02, thus meeting the requirements for mapmaking [39].
- (3) Shape measures of the roads: Shape measures include the number of bends, the number of extremal points, and the curvature [40]. A comparison of these three shape measures of these roads in this experiment is shown in Figure 16. In Figure 16, A represents the number of shape measures of road objects after resolving road graphic conflicts, and B represents the number of shape measures of the original road objects.  $|1 - A/B|$  can explain the degree of change in these three indicators, which was 0.0491, 0.0644, and 0.0461, respectively, in this experiment; these values were very small.



**Figure 16.** Comparison of road shape measures. The values on the horizontal axis represent the shape measure of the road objects after and before resolving road graphic conflicts. The values on the vertical axis represent the number of shape measures.

#### 4. Conclusions

The collaborative methods proposed in this study can effectively resolve road graphic conflicts and are guided by cartographic rules. Based on the characteristics of road graphic conflict areas, three collaborative methods were designed to deal with different types of road graphic conflicts: collaboration between deletion and the snake displacement model, collaboration between the snake displacement model and collinearity, and collaboration among simplification, smoothing, and the beam displacement model. Qualitative and quantitative analyses of the experimental results showed the proficiency of these collaborative methods in resolving road graphic conflicts. The road shape features were adequately maintained.

These new methods for resolving road graphic conflicts should be further researched while considering geospatial contextual information, such as the spatial relationships between roads and other map features. More types of graphic conflicts between roads and other map features should be considered, and more collaborative methods for resolving these new graphic conflicts need to be investigated.

**Author Contributions:** Methodology, Chuanbang Zheng, Qingsheng Guo and Lin Wang; validation, Chuanbang Zheng and Qingsheng Guo; formal analysis, Lin Wang and Yuangang Liu; investigation, Jianfeng Jiang; data curation, Yuangang Liu and Jianfeng Jiang; writing—original draft, Chuanbang Zheng; writing—review & editing, Qingsheng Guo. All authors have read and agreed to the published version of the manuscript.

**Funding:** This research was funded by the National Natural Science Foundation of China (No. 41871378).

**Data Availability Statement:** The data presented in this study are publicly available at <https://www.openstreetmap.org/> (accessed on 2 May 2024).

**Conflicts of Interest:** The authors declare no conflicts of interest.

## References

1. Yang, M.; Cheng, L.; Cao, M.; Yan, X. A Stacking Ensemble Learning Method to Classify the Patterns of Complex Road Junctions. *ISPRS Int. J. Geo-Inf.* **2022**, *11*, 523. [CrossRef]
2. Yang, M.; Jiang, C.; Yan, X.; Ai, T.; Cao, M.; Chen, W. Detecting interchanges in road networks using a graph convolutional network approach. *Int. J. Geogr. Inf. Sci.* **2022**, *36*, 1119–1139. [CrossRef]
3. Courtial, A.; Touya, G.; Zhang, X. Deriving map images of generalised mountain roads with generative adversarial networks. *Int. J. Geogr. Inf. Sci.* **2023**, *37*, 499–528. [CrossRef]
4. Touya, G. A road network selection process based on data enrichment and structure detection. *Trans. GIS* **2010**, *14*, 595–614. [CrossRef]
5. Han, Y.; Wang, Z.; Lu, X.; Hu, B. Application of AHP to road selection. *ISPRS Int. J. Geo-Inf.* **2020**, *9*, 86. [CrossRef]
6. Guo, Q.; Wang, H.; He, J.; Zhou, C.; Liu, Y.; Xing, B.; Jia, Z.; Li, M. Graphic simplification and intelligent adjustment methods of road networks for navigation with reduced precision. *ISPRS Int. J. Geo-Inf.* **2020**, *9*, 490. [CrossRef]
7. Baur, L.; Funke, S.; Rupp, T.; Störandt, S. Gradual road network simplification with shape and topology preservation. In Proceedings of the 30th International Conference on Advances in Geographic Information Systems, Seattle, WA, USA, 1–4 November 2022; pp. 1–4. [CrossRef]
8. Balboa, J.L.G.; López, F.J.A. Sinuosity pattern recognition of road features for segmentation purposes in cartographic generalization. *Pattern Recognit.* **2009**, *42*, 2150–2159. [CrossRef]
9. Bader, M. Energy Minimization Methods for Feature Displacement in Map Generalization. Ph.D. Thesis, University of Zurich, Zürich, Switzerland, 2001.
10. Liu, Y. Research and Improvement of Cartographic Displacement Algorithms Based on Energy Minimization Principles. Ph.D. Thesis, Wuhan University, Wuhan, China, 2015.
11. Touya, G.; Lokhat, I. ReBankment: Displacing embankment lines from roads and rivers with a least squares adjustment. *Int. J. Cartogr.* **2022**, *8*, 37–53. [CrossRef]
12. Ruas, A. Modèle de généralisation de données géographiques à base de contraintes et d'autonomie. Ph.D. Thesis, Université de Marne-la-Vallée, Paris, France, 1999.
13. Stanislawski, L.V.; Bottenfield, B.P.; Bereuter, P.; Savino, S.; Brewer, C.A. Generalisation operators. In *Abstracting Geographic Information in a Data Rich World: Methodologies and Applications of Map Generalization*; Springer International Publishing: Cham, Switzerland, 2014; pp. 157–195. [CrossRef]
14. Ai, T. A displacement of building cluster based on field analysis. *Acta Geod. Et Cartogr. Sin.* **2004**, *33*, 89–94.
15. Burghardt, D.; Meier, S. Cartographic displacement using the snakes concept. In *Semantic Modeling for the Acquisition of Topographic Information from Images and Maps*; Birkhäuser Verlag: Basel, Switzerland, 1997; pp. 59–71.
16. Wang, L.; Guo, Q.; Wei, Z.; Liu, Y. Spatial conflict resolution in a multi-agent process by the use of a snake model. *IEEE Access* **2017**, *5*, 24249–24261. [CrossRef]
17. Wang, L. Collaborative Displacement Method of Multi-Feature Based on Multi-Agent System. Ph.D. Thesis, Wuhan University, Wuhan, China, 2018.
18. Wei, Z.; Ding, S.; Xu, W.; Cheng, L.; Zhang, S.; Wang, Y. Elastic beam algorithm for generating circular cartograms. *Cartogr. Geogr. Inf. Sci.* **2023**, *50*, 371–384. [CrossRef]
19. Wei, Z.; He, J.; Wang, L.; Wang, Y.; Guo, Q. A collaborative displacement approach for spatial conflicts in urban building map generalization. *IEEE Access* **2018**, *6*, 26918–26929. [CrossRef]
20. Huang, H.; Guo, Q.; Sun, Y.; Liu, Y. Reducing building conflicts in map generalization with an improved PSO algorithm. *ISPRS Int. J. Geo-Inf.* **2017**, *6*, 127. [CrossRef]
21. Nickerson, B.G. Automated cartographic generalization for linear features. *Cartogr. Int. J. Geogr. Inf. Geovisualization* **1998**, *25*, 15–66. [CrossRef]
22. Fei, L. Solving graphic conflicts between streets and buildings in map compilation by simulating human cartographers. *Geomat. Inf. Sci. Wuhan Univ.* **2004**, *29*, 426–432. [CrossRef]
23. Ware, J.M.; Jones, C.B. Conflict Reduction in Map Generalization Using Iterative Improvement. *GeoInformatica* **1998**, *2*, 383–407. [CrossRef]
24. Ware, J.M.; Jones, C.B.; Thomas, N. Automated map generalization with multiple operators: A simulated annealing approach. *Int. J. Geogr. Inf. Sci.* **2003**, *17*, 743–769. [CrossRef]
25. Wu, F.; Du, J.; Qian, H.; Zhai, R. Overview of Research Progress and Reflections in Intelligent Map Generalization. *Geomat. Inf. Sci. Wuhan Univ.* **2022**, *47*, 1675–1687. [CrossRef]
26. Duchêne, C.; Ruas, A.; Cambier, C. The CartACom model: Transforming cartographic features into communicating agents for cartographic generalisation. *Int. J. Geogr. Inf. Sci.* **2012**, *26*, 1533–1562. [CrossRef]

27. Renard, J.; Duchêne, C. Urban structure generalization in multi-agent process by use of reactive agents. *Trans. GIS* **2014**, *18*, 201–218. [[CrossRef](#)]
28. Yan, J.; Guilbert, E.; Saux, E. An ontology-driven multi-agent system for nautical chart generalization. *Cartogr. Geogr. Inf. Sci.* **2017**, *44*, 201–215. [[CrossRef](#)]
29. Boodala, J.; Dikshit, O.; Balasubramanian, N. Automated generalisation of buildings using CartAgen platform. *arXiv* **2022**, arXiv:2204.01544. [[CrossRef](#)]
30. Touya, G.; Lokhat, I.; Duchêne, C. CartAgen: An open source research platform for map generalization. *Proc. ICA Copernic. GmbH* **2019**, *2*, 134. [[CrossRef](#)]
31. Touya, G.; Duchêne, C.; Taillandier, P.; Gaffuri, J.; Ruas, A.; Renard, J. Multi-Agents Systems for Cartographic Generalization: Feedback from Past and On-Going Research. Ph.D. Thesis, IGN (Institut National de l'Information Géographique et Forestière), Paris, France, 2018.
32. Li, W.; Yan, H.; Lu, X.; Shen, Y. A Heuristic Approach for Resolving Spatial Conflicts of Buildings in Urban Villages. *ISPRS Int. J. Geo-Inf.* **2023**, *12*, 392. [[CrossRef](#)]
33. Wu, F.; Gong, X.; Du, J. Overview of the research progress in automated map generalization. *Acta Geod. Et Cartogr. Sin.* **2017**, *46*, 1645. [[CrossRef](#)]
34. Poorten, P.V.D.; Jones, C.B. Characterisation and generalisation of cartographic lines using Delaunay triangulation. *Int. J. Geogr. Inf. Sci.* **2002**, *16*, 773–794. [[CrossRef](#)]
35. Ai, T.; Ke, S.; Yang, M.; Li, J. Envelope generation and simplification of polylines using Delaunay triangulation. *Int. J. Geogr. Inf. Sci.* **2017**, *31*, 297–319. [[CrossRef](#)]
36. Li, Z. *Algorithmic Foundation of Multi-Scale Spatial Representation*; CRC Press: Boca Raton, FL, USA, 2006. [[CrossRef](#)]
37. Regnauld, N.; McMaster, R.B. A synoptic view of generalisation operators. In *Generalisation of Geographic Information*; Elsevier Science BV: Amsterdam, The Netherlands, 2007; pp. 37–66. [[CrossRef](#)]
38. National Administration of Surveying, Mapping and Geoinformation of China. *Compilation Specification for National Fundamental Scale Maps-Part1: Compilation Specifications for 1:25,000, 1:50,000 & 1:100,000 Topographic Maps*; China Zhijian Publishing House: Beijing, China, 2008.
39. Duchêne, C. *Individual Road Generalisation in the 1997–2000 AGENT European Project*; Technical Report; IGN, COGIT lab: Paris, France, 2014.
40. Jiang, J.; Guo, Q.; Wang, Y.; Zheng, C.; Zhong, Q. Progressive simplification of bends of lines with multi-constraints. *Sci. Surv. Mapp.* **2023**, *48*, 212–221.

**Disclaimer/Publisher's Note:** The statements, opinions and data contained in all publications are solely those of the individual author(s) and contributor(s) and not of MDPI and/or the editor(s). MDPI and/or the editor(s) disclaim responsibility for any injury to people or property resulting from any ideas, methods, instructions or products referred to in the content.